Article

Improvement on penetration of liner shaped charges: Evaluation by 2D and 3D simulation

Hitoshi Miyoshi*, Hiromichi Ohba**, Hideki Kitamura**, Tatsuya Inoue**, and Tetsuyuki Hiroe***

*Project Division, Chugoku Kayaku Co., Ltd., 4-5-14 Nihonbashi-honcho, Chuo-ku, Tokyo, JAPAN
e-mail: miyoshi@chugokukayaku.co.jp

**Yoshii Plant, Chugoku Kayaku Co., Ltd., 2530 Iwasaki, Yoshii-mach, Gunma 370-2131, JAPAN

***Department of Mechanical Engineering and Materials Science, Kumamoto University, 2-39-1 Kurokami, Kumamoto 860-8555, JAPAN
e-mail: hiroe@gpo.kumamoto-u.ac.jp

Received: May 27, 2005 Accepted: July 4, 2005

Abstract

Experiments and simulations of linear shaped charges (LSCs) have been conducted to improve the penetration performance and minimize collateral damage by fragments. Annealed tough pitch copper was selected for an appropriate liner material. The penetration depth increased by 50 %, compared to current LSCs. The detonation effects of explosives change the liner into the jet and slug. But, the case is transformed into fragments, which set up undesirable damages. Polyvinyl chloride was adopted as the case material to reduce damage by fragments. No fragments were generated when the newly-designed LSCs were shot. With AUTODYN, the Euler solver for 2D calculation and the SPH (smoothed particle hydrodynamics) and Lagrange solver for the 3D were adopted. From the simulations, the process of the penetration was verified and the slug with high velocity seems to have the ability of penetration. The jet profile was confirmed by the 3D simulation of the SPH solver.

Keywords: Linear shaped charges, Target penetration, Stand-off distance, SPH solver

1. Introduction

Liner shaped charges (LSCs) have the ability for the instantaneous cutting of the structures and have been used in the separation between the first and second stages, and the command destruction of solid rocket boosters (SRB) in the H-2A rocket. In the civil engineering field, LSCs have been used in the demolition of the big structures such as buildings, iron bridges and cranes.

The penetration performance of conical shaped charges (CSCs) is usually 8.0 times of the cone diameter (CD) at the best configurations, while LSCs have performance at 1.2 times of the charge width at a maximum. Improvement of the penetration performance is needed to conduct an effective cutting.

Appropriate setting of the stand-off, which is a distance between the liner base part of LSCs and the surface of the target, needs to be controlled to obtain the optimal penetration performance.

The collateral damage by the fragments from the case part of LSCs should be eliminated to conduct the cutting plans reliably and safely.

Authors presented that simulations by using AUTODYN are useful for understanding the process of jet formation and target penetration[1]. The modeling and simulation for the jet formation and penetration of LSCs are essential, because the understanding of these phenomena is needed to evaluate as the two- and three-dimensional (2D & 3D) moving. The Euler solver for 2D calculation, and the SPH (Smoothed particle hydrodynamics) and the Lagrange solver for 3D were adopted.

In this paper, we present our effort for improving the penetration performance, minimizing fragments and obtaining an appropriate stand-off. The 2D and 3D simulation results gave us a lot of information about determining our objects.

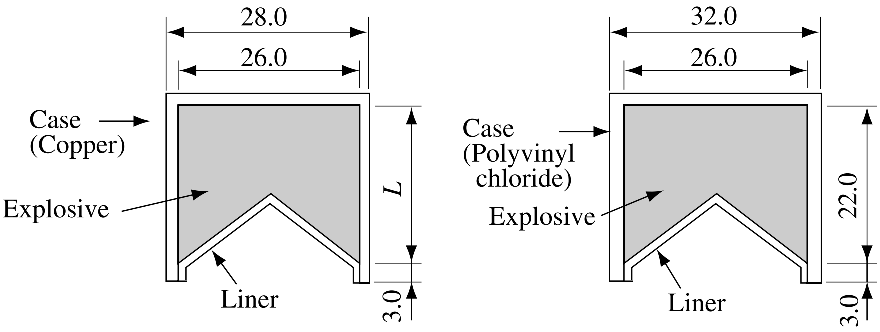

Fig. 1 Dimensions of LSCs.

2. Design and manufacture

2.1 Liner and case

The manufacturing method of LSCs exists two types, the press and cast loading type. The press loading type LSCs were tested and evaluated in our previous paper[1]. In order to enhance the penetration performance of LSCs, the cast loading type is suitable, because it is easy to modify the shape of the liner, to optimize the particle distribution of the liner material, and to adjust the explosive weight.

LSCs consist of the liner, case and explosive, as shown in Fig. 1. Copper is usually adopted as a material of the liner. A tough pitch copper plate was cut to the required dimensions for the liner and case. The copper plates were angled at prescribed forms.

Dimensional accuracy was acceptable, but the remaining stress due to the bending work was anticipated. Annealing conditions were at 400 degree C for two hours in a vacuum. Assembly of the liner and case was conducted by two methods; silver brazing and soldering. Treated temperature is about 750 and 250 degree C, respectively. The temperature of the silver brazing method is too high to invalidate the annealing effect. Since the recrystallization temperature of copper is 650 degree C, the silver brazing makes the particle size of copper larger and constitutes a limiting factor of the good jet formation and the troublesome jet break-up. The specimens from the soldering were expected to lead to good penetration results and were used for the first step experiment, the stand-off test.

In order to reduce damage by fragments, polyvinyl chloride was adopted as the case material. Two types of LSCs were manufactured, that is, a copper case type (CC) and a reduced fragments (RF) type.

2.2 Explosive loading

During initial phases of explosive loading, octol 75/25 was planed, but small gas bubbles in the explosive were not able to be removed. Defoaming and warming in vacuum were ineffective. Therefore, octol 70 / 30 was loaded.

Copper case types were loaded with explosives, and then defoamed and warmed in a vacuum. Small gas bubbles were approximately able to be removed. After gradually cooling and solidification, small porosities were generated.

Warming in a vacuum was not structurally applied to the reduced fragments type. Loading in the atmosphere was conducted, and the explosive was gradually cooled and became solidified. Gas bubbles and porosities were hardly

Table 1 Explosive loading data.

LSC type	Charge height (mm)	Mass (g)	Explosive weight (g)	Explosive density (g cm^{-3})	Remarks
CC-A-1	31	473	228	1.80	
CC-A-2		474	230	1.81	
CC-A-3		472	229	1.80	
CC-B-1	26	406	180	1.80	
CC-B-2		409	183	1.83	
CC-B-3		413	189	1.87	Case became deformed
CC-C-1	21	341	134	1.80	
CC-C-2		342	134	1.80	
CC-C-3		---	---	---	Measurement mistake
RF-1	22	274	148	---	Density was not calculated
RF-2		282	157	---	
RF-3		271	146	---	

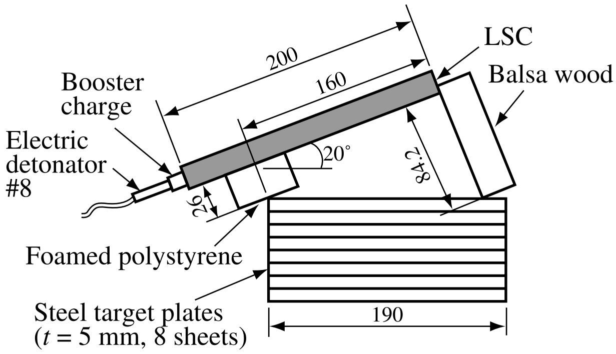

Fig. 2 Stand-off test setup.

observed at all.

Explosive loading data of LSCs is shown in Table 1. The final number 2 in the LSC type means the soldering method, and all the others used silver brazing. All of LSCs were 200 mm in length.

3. Experiments

3.1 Stand-off test

The aim of the test is to obtain the relationship between the stand-off distance and the penetration depth, and to therefore determine the optimal stand-off distance.

Determination of an appropriate stand-off distance is very important to obtain high cutting performance of LSCs. Figure 2 shows the setup of the stand-off test. From the items showed in table 1, CC-A-2, CC-B-2, CC-C-2, and RF-2 were selected for testing.

3.2 Fragmentation test

The aim of the test is to observe the damage of the witness plate in case of the polyvinyl case, compared to the copper case. Two witness steel plates, 3.2 and 1.6 mm thick, were placed at 2 m point from a LSC.

3.3 Penetration test

The penetration performance of LSCs against the steel targets was evaluated by using the data from the stand-off test, and the fragmentation test was conducted at the same moment. The setup of the penetration test was similar to Fig. 2, except that a LSC was placed parallel to the steel target plates.

These tests were conducted in the dome-type explosion test facility, located in the Yoshii plant. The facility has the enclosed space of 8 m in diameter and 5 m in height and the inner wall consists of reinforced concrete several meters thick, steel plate 25 mm thick, and three steel plate 3.2 mm thick for protection from fragments and blast waves.

4. Results

4.1 Stand-off test

4.1.1 Calculation of the jet velocity

When the target is penetrated by the jet, some vestiges generated by the jet are observed, as shown in Fig. 3. When the velocity of the jet front and the detonation velocity are represented as V_j and U, respectively, the equation (1) was obtained.

$$\sin\theta = V_j / U \tag{1}$$

From Fig. 3, the penetration angle is shown in the equation (2), and the jet velocity is represented as the equation (3).

$$\theta = \frac{\pi}{2} - \alpha - \beta \tag{2}$$

$$V_j = U \cos(\alpha + \beta) \tag{3}$$

From the experiments, the angle is 47 degree, and the detonation velocity is 8,400 m/s. By using the equation (1), the jet velocity was calculated to be about 3,300 $\mathrm{ms^{-1}}$.

4.1.2 Maximum penetration point

The explanation drawing of the optimal stand-off calculation is shown in Fig. 4. The optimal stand-off S is calculated by using the equation (4) and (5).

$$L = \frac{(h + P)\cos\alpha}{\cos\theta} - \frac{P}{\cos(\alpha + \theta)} \tag{4}$$

$$S = L\cos\theta \tag{5}$$

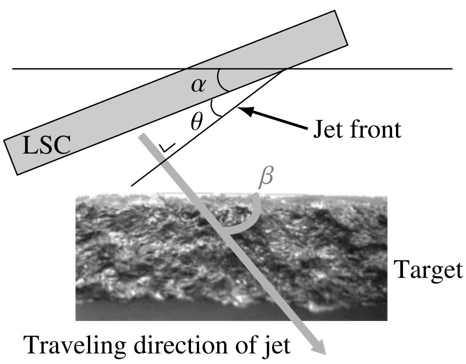

Fig. 3 Calculation of the jet velocity.

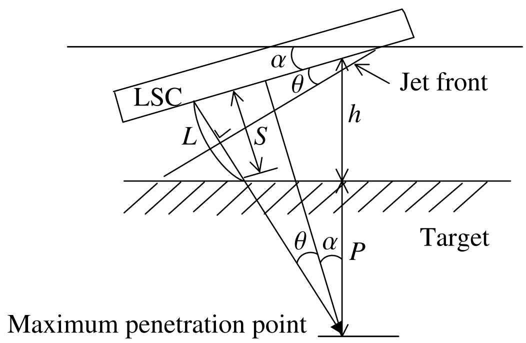

Fig. 4 Explanation chart of the optimal stand-off calculation.

From the test results, the most appropriate part of the penetration was determined to be located at about 69 mm from the left end of the steel target. The parameter of the equation (4) and (5) was obtained, that is, h is 50 mm, P 30 mm, alpha 20 degree and theta 23 degree. Therefore, the optimal stand-off was determined to be 40mm.

4.2 Fragmentation test

As shown in Fig. 5, no fragments were generated when the reduced fragments type was shot. Contrary, to take a single example, a copper case type generates 141 penetration holes on a steel plate 1.6 mm thick, and 87 holes on a plate 3.2 mm thick.

4.3 Penetration test

The test results were shown in Table 2. The penetration 76 holes of CC-A-1* were not complete, because the plate was not correctly set. A few pieces of holes of RF-1** were generated by the fragments from the target cutting. In case of RF-3***, the fragments from the target were deflected by some wood boards.

5. 2D and 3D simulations

Simulations were conducted with AUTODYN-2D & 3D to verify the optimal stand-off and the maximum penetration depth.

The Euler solver on the 2D planar was selected, and the liner, case, explosive, air, and steel target were filled on the Euler solver plane. The number of the mesh division was 200 times 300, and the mesh density was increased in the center of the plane, where explosive was filled. For the copper liner and copper case, the shock Hugoniot equation of state (EOS) and Steinberg-Guinan strength model, and for the steel target, the shock Hugoniot EOS and Johnson-Cook strength model were applied. For the explosive the JWL EOS, and air the Ideal gas EOS were applied. For the RF type, we substituted polyethylene for polyvinyl chloride, since polyvinyl chloride was not registered in the data library of AUTODYN. The EOS of polyethylene was applied the shock Hugoniot EOS.

Figure 6 shows the snap shots at 0, 15.4, 21.4, 33.2 and 73.4 micro-second from the mpeg file of CC-B type. The charge height, stand-off distance, and target thickness were changed in concert with the setup of the experiments.

Using the SPH (Smoothed particle hydrodynamics) solver for evaluating of the shaped charge phenomena was proposed[2), 3)]. The SPH and Lagrange solver were adopted to conduct the 3D simulation of LSCs.

The Lagrange solver is adopted for the case, explosive and target, and the SPH solver for the liner. The EOS of the case, liner, explosive and target were the same as the 2D simulation. The SPH model was produced by using the Lagrange solver in the first stage, because the AUTODYN don't support the modeling of complicated shapes. The Lagrange model built was converted to the SPH model, and 0.5 mm in diameter of the SPH particle size was selected. The length of the modeling of the LSC was 50 mm. The number of the SPH particles is 8,500, and the number of mesh division of explosive 540,800 and case 4,300. The axial symmetry model was not adopted because the SPH solver doesn't give the correct calculation results[3)]. The jet formation, jet stretch process and penetration in the first step were observed the 3D simulation results, as shown in Fig. 7. The snap shots at 3.2, 7.3, 12.6, 14.9 and 17.2 micro-second were extracted from a mpeg file, but the explosive

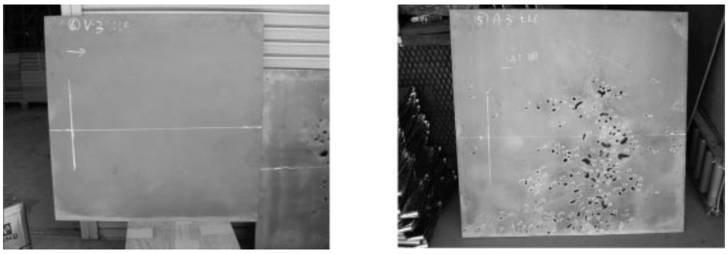

Fig. 5 Zero and 141 holes on the witness plates.

Table 2 Results of the fragmentation and penetration test.

LSC	Charge height (mm)	Target (mm)	Cutting result	Steel plate (mm)/ Penetration holes (pcs)
CC-A-1	31	35	Complete cut by penetration	1.6 / 136, 3.2 / 76*
CC-A-3		40	Complete cut by penetration	1.6 / 141, 3.2 / 87
CC-B-1	26	35	Complete cut, but rupture of small part	1.6 / 104, 3.2 / 53
CC-B-3		40	Complete cut by penetration	1.6 / 108, 3.2 / 38
CC-C-1	21	35	Complete cut, but rupture of small part	1.6 / 64, 3.2 / 34
CC-C-3		40	Incomplete cut at detonation point	1.6 / 78, 3.2 / 53
RF-1	22	25	Complete cut, but rupture of large part	1.6 / 2, 3.2 / 5**
RF-3		30	Complete cut, but rupture of large part	1.6 / 0, 3.2 / 0***

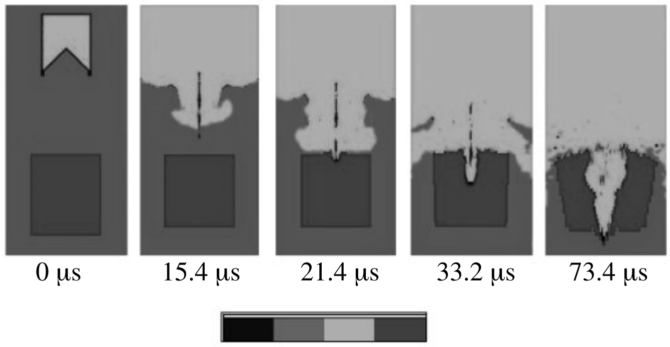

Fig. 6 Penetration simulation on 2D.

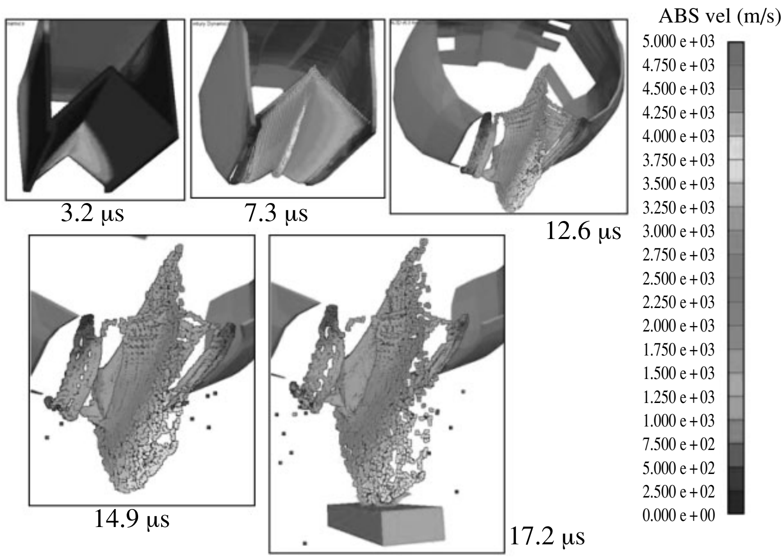

Fig. 7 Jet formation simulation on 3D.

part leaves out from the shots, because the wide spread of the detonation products bescreens the liner and case.

6. Discussions

The jet and slug tip velocity corresponding to the distance from the liner base were obtained from the 2D simulations, as shown Fig. 8. The average jet velocity was determined to be about 3,500 ms^{-1}. The result agrees with our assumption showing in 4.1.1.

The penetration depth was compared with experiments and calculations. The maximum penetration depth was estimated to be 47 mm on a CC-A type LSC and was equivalent to 1.81 times of the charge width, 26 mm. As the maximum penetration depth of a current LSC is 1.2 times at a maximum, the one of the newly-designed LSC increased by about 50 %.

Stand-off effects were clearly confirmed by the simulations. The optimal stand-off was determined to be 40 mm and a series of experiments was conducted with use of this data. For the type CC-B, the penetration depth was calculated to be 43.5 mm. When the stand-off was set as 20 and 40 mm, the penetration depth was calculated to be 29.0 and 21.6 mm, respectively.

The penetration velocity profile was also obtained from the simulations and two-step penetration process was confirmed. For the type CC-A, two-third thickness of the target steel was penetrated by the jet and the residue was decoupled by the slug. As shown in Fig. 9, the slug has the velocity of more than 2000 m s^{-1}, and has the ability for cutting the steel target.

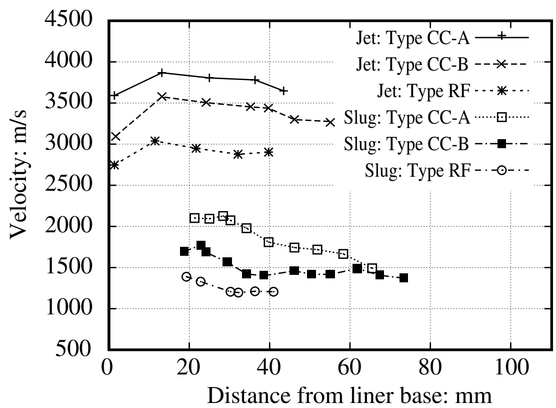

Fig. 8 Jet and slug tip velocity.

By changing copper into polyvinyl chloride, the generation of fragments from the case was completely inhibited. The reduced fragment type LSCs have a highly utility value at a cutting work, when some fragile and expensive

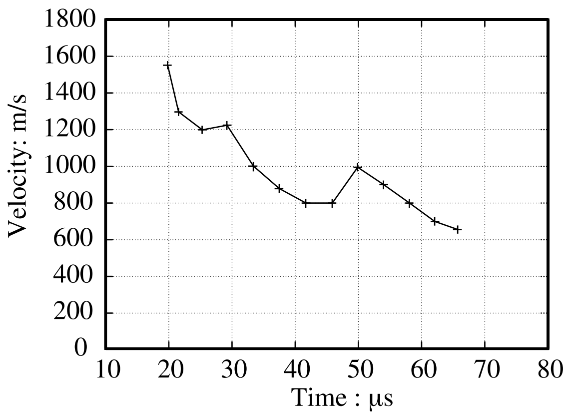

Fig. 9 Penetration velocity profile.

things are located nearby. As polyvinyl chloride has no confinement effects, lowering of the penetration depth was estimated. Experimental results have a slight difference between the CC-C type and RF type. Additional experiments and simulations should be conducted to evaluate the confinement effects.

Explosive loading for a narrow and long space was crucial, because the penetration performance is influenced a great deal by precise loading conditions. Special loading tools should need to ascertain equable condition of explosives.

The 2D simulation gives us the maximum penetration depth at the optimal stand-off distance, but the understanding of the jet profile is very difficult, because the jet is only described as one single line, as shown in Fig. 6. The 2D planar model is represented the propagation of the detonation as the linear detonation happens all at once.

From the 3D simulation, the propagation of detonation wave, the jet formation, the jet elongation and the penetration were observed. The SPH particles showed visually and precisely the temporal change in the jet. The shot at 14.9 microsecond shows that some faster parts of the jet exist right after the jet tip by observing more reddish particle. The phenomena are accountable for the theory of the jet formation.

The simulation of the overall penetration process is not conducted at this time. Some techniques on the calculation are needed to progress the simulation, including the modification of the mesh conditions, the deletion of unneeded parts, and the adjustment of material parameters.

7. Conclusions

The stand-off test, fragmentation test and penetration test were conducted, and the 2D and 3D simulations by using AUTODYN were also carried out. We have come to the conclusions through the present study as follows:

1) The procedures for obtaining the optimal stand-off distance were confirmed.
2) Adopting polyvinyl chloride for the case material drastically decreases fragments from the case.
3) The ability for penetration of the slug with high velocity was confirmed.
4) 2D simulations based on the experimental results indicate that newly-designed LSCs have 1.5 times penetration ability, compared to current products.
5) 3D simulations by using the SPH solver demonstrate the formation and elongation process of the jet.

The simulations by using AUTODYN must be used for designing the effective cutting plans for use with LSCs.

References

1) H. Miyoshi, H. Ohba, E. Kuroiwa, T. Inoue, H. Kitamura and T. Hiroe, The jet penetration performance of linear shaped charges, Science and Technology of Energetic Materials, 65, 339, pp. 173-179, 2004 (in Japanese).
2) Katsumi Tanaka, SPH (Smoothed Particle Hydrodynamics) Analysis of Jetting by Shaped Charge, Proceedings of an Academic Meeting of the Japan Explosive Society (autumn), pp. 59-60, November 2004 (in Japanese).
3) Katsumi Tanaka, SPH Studies of Crater by Explosion and Shock Wave Phenomena, Proceedings of Symposium on Shock Wave Japan FY 2004, pp. 185-186, Sendai, March 2005 (in Japanese).

2次元および3次元シミュレーションを活用した リニアシェイプトチャージ(LSC)の侵徹性能向上

三好　仁*，大羽博通**，北村秀樹**，井上達也**，廣江哲幸***

リニアシェイプトチャージ(LSC)の侵徹性能向上と破片生成低減に関する研究を行った。侵徹性能に関しては，ライナに熱処理したタフピッチ銅を使うことで50%の威力向上が得られた。また，ケースの材質を銅から塩ビに変えることで破片生成が皆無にできた。2次元Eulerと3次元SPH，Lagrange solverを使ったシミュレーションで試験結果の的確な評価できた。特に，高速のスラグも侵徹能力があることが確認できた。また，SPH solverを採用することにより，LSCジェットの3次元挙動が把握できるようになった。

*中国化薬(株)企画部　〒103-0023　東京都中央区日本橋本町4-5-14入江ビル
e-mail: miyoshi@chugokukayaku.co.jp

**中国化薬(株)吉井工場　〒370-2131　群馬県多野郡吉井町岩崎2530

***熊本大学工学部　〒860-8555　熊本市黒髪2-39-1
e-mail: hiroe@gpo.kumamoto-u.ac.jp